

ARMY RESEARCH LABORATORY

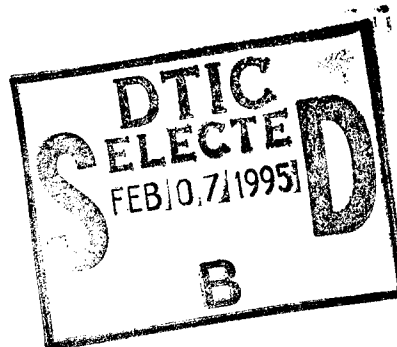


# Computational Fluid Dynamics (CFD) Simulation of Test Chamber and Smoke-Generating Device

Michael J. Nusca

ARL-TR-663

January 1995



19950131 024

APPROVED FOR PUBLIC RELEASE; DISTRIBUTION IS UNLIMITED.

## **NOTICES**

**Destroy this report when it is no longer needed. DO NOT return it to the originator.**

**Additional copies of this report may be obtained from the National Technical Information Service, U.S. Department of Commerce, 5285 Port Royal Road, Springfield, VA 22161.**

**The findings of this report are not to be construed as an official Department of the Army position, unless so designated by other authorized documents.**

**The use of trade names or manufacturers' names in this report does not constitute endorsement of any commercial product.**

# REPORT DOCUMENTATION PAGE

Form Approved  
OMB No. 0704-0188

Public reporting burden for this collection of information is estimated to average 1 hour per response, including the time for reviewing instructions, searching existing data sources, gathering and maintaining the data needed, and completing and reviewing the collection of information. Send comments regarding this burden estimate or any other aspect of this collection of information, including suggestions for reducing this burden, to Washington Headquarters Services, Directorate for Information Operations and Reports, 1215 Jefferson Davis Highway, Suite 1204, Arlington, VA 22202-4302, and to the Office of Management and Budget, Paperwork Reduction Project (0704-0188), Washington, DC 20503.

1. AGENCY USE ONLY (Leave blank)		2. REPORT DATE January 1995	3. REPORT TYPE AND DATES COVERED Final, December 1993–August 1994	
4. TITLE AND SUBTITLE Computational Fluid Dynamics (CFD) Simulation of Test Chamber and Smoke-Generating Device			5. FUNDING NUMBERS PR: 1L162618A1FL	
6. AUTHOR(S) Michael J. Nusca				
7. PERFORMING ORGANIZATION NAME(S) AND ADDRESS(ES) U.S. Army Research Laboratory ATTN: AMSRL-WT-PA Aberdeen Proving Ground, MD 21005-5066			8. PERFORMING ORGANIZATION REPORT NUMBER	
9. SPONSORING/MONITORING AGENCY NAME(S) AND ADDRESS(ES) U.S. Army Research Laboratory ATTN: AMSRL-OP-AP-L Aberdeen Proving Ground, MD 21005-5066			10. SPONSORING/MONITORING AGENCY REPORT NUMBER ARL-TR-663	
11. SUPPLEMENTARY NOTES				
12a. DISTRIBUTION/AVAILABILITY STATEMENT Approved for public release; distribution is unlimited.			12b. DISTRIBUTION CODE	
13. ABSTRACT (Maximum 200 words)  The U.S. Army Research Laboratory (ARL) has completed an initial investigation of the flow field within a typical U.S. Army Edgewood Research, Development, and Engineering Center (ERDEC) test chamber via numerical simulation. The ERDEC test chamber is designed to mix compressor-driven airflow with gas/solid effluent from a test article placed inside the chamber. An example of such a test article is a smoke generator, or smoke pot. Simulation of this flow utilized ARL computational fluid dynamics (CFD) codes that include multispecies chemical kinetics. Numerical solutions of the gas flow and effluent concentration distributions in the test chamber were generated for operating times up to 4.5 min. Numerical simulations reveal that certain values of chamber through-flow induce flow patterns within the chamber that are dominated by rotating vortices. This flow pattern increases the effluent residence time in the chamber as well as the mixing of gas/particulate from the test article with air. As a result, pockets of high effluent concentration can form in the chamber. Graphical results with discussion are presented.				
14. SUBJECT TERMS Navier-Stokes, computational fluid dynamics, turbulence, smoke, obscurants			15. NUMBER OF PAGES 35	
			16. PRICE CODE	
17. SECURITY CLASSIFICATION OF REPORT UNCLASSIFIED	18. SECURITY CLASSIFICATION OF THIS PAGE UNCLASSIFIED	19. SECURITY CLASSIFICATION OF ABSTRACT UNCLASSIFIED	20. LIMITATION OF ABSTRACT SAR	

INTENTIONALLY LEFT BLANK.

## ACKNOWLEDGMENTS

Mr. Don Palughi and Mr. Larry Bickford of the Research and Technology Directorate of the U.S. Army Edgewood Research, Development, and Engineering Center (ERDEC) are acknowledged for supporting this effort and for providing technical assistance.

Accession For	
NTIS GRA&I	<input checked="checked" type="checkbox"/>
DTIC TAB	<input type="checkbox"/>
Unannounced	<input type="checkbox"/>
Justification	
By	
Distribution	
Availability Codes	
Dist	Avail and/or Special

INTENTIONALLY LEFT BLANK.

## TABLE OF CONTENTS

	<u>Page</u>
ACKNOWLEDGMENTS .....	iii
LIST OF FIGURES .....	vi
1. INTRODUCTION .....	1
2. GOVERNING EQUATIONS .....	1
3. BOUNDARY CONDITIONS AND INITIAL CONDITIONS .....	5
4. COMPUTATIONAL ALGORITHM .....	5
5. RESULTS AND DISCUSSION .....	6
6. CONCLUSIONS .....	7
7. REFERENCES .....	25
LIST OF SYMBOLS .....	27
DISTRIBUTION LIST .....	29

INTENTIONALLY LEFT BLANK.



## LIST OF FIGURES

<u>Figure</u>	<u>Page</u>
1. Schematic of test chamber and smoke pot showing computational grid . . . . .	8
2. Stream function contours before smoke pot operation . . . . .	9
3. Stream function contours 1.0 min after smoke pot startup . . . . .	10
4. Stream function contours 2.0 min after smoke pot startup . . . . .	11
5. Stream function contours 3.0 min after smoke pot startup . . . . .	12
6. Stream function contours 4.0 min after smoke pot startup . . . . .	13
7. Stream function contours 4.5 min after smoke pot startup, 0.5 min after smoke pot termination . . . . .	14
8. Effluent mass fraction contours 1.0 min after smoke pot startup . . . . .	15
9. Effluent mass fraction contours 2.0 min after smoke pot startup . . . . .	16
10. Effluent mass fraction contours 3.0 min after smoke pot startup . . . . .	17
11. Effluent mass fraction contours 4.0 min after smoke pot startup . . . . .	18
12. Effluent mass fraction contours 4.5 min after smoke pot startup, 0.5 min after smoke pot termination . . . . .	19
13. Effluent density ( $\text{g/m}^3$ ) contours 1.0 min after smoke pot startup . . . . .	20
14. Effluent density ( $\text{g/m}^3$ ) contours 2.0 min after smoke pot startup . . . . .	21
15. Effluent density ( $\text{g/m}^3$ ) contours 3.0 min after smoke pot startup . . . . .	22
16. Effluent density ( $\text{g/m}^3$ ) contours 4.0 min after smoke pot startup . . . . .	23
17. Effluent density ( $\text{g/m}^3$ ) contours 4.5 min after smoke pot startup, 0.5 min after smoke pot termination . . . . .	24

INTENTIONALLY LEFT BLANK.

## 1. INTRODUCTION

The U.S. Army Research Laboratory (ARL) completed an initial investigation of the flow field within a typical test chamber operated by the Army Edgewood Research, Development and Engineering Center (ERDEC). The ERDEC test chamber is designed to mix compressor-driven airflow with gas/solid effluent from a test article placed inside the chamber. An example of such a test article is a smoke generator, or smoke pot, commonly used on the battlefield to provide a means of obscurant. During the test, the air/effluent flow field is exhausted from the test chamber for analysis. In order to simulate this flow, the ARL applied computational fluid dynamics (CFD) codes that include multispecies chemical kinetics as well as multiphase (particulate) submodels. These codes were developed at ARL to numerically solve the Navier-Stokes equations and simulate the chemically reacting, multiphase flow field in gun propulsion systems. This code has been used successfully for other applications at ARL (Nusca 1989, 1991, 1993).

Application of the code to the present study involved generating a computational mesh that covered the chamber interior as well as specifying proper boundary conditions on the chamber walls, chamber top (air inflow), chamber exit (outflow), and test article (effluent outflow), as depicted in Figure 1. The governing equations, boundary conditions, and solution method are outlined in this report. Numerical solutions of the gas flow and effluent concentration distributions in the test chamber were generated for operating times up to 4.5 min. Graphical results with discussion are presented in this report. Numerical simulations reveal that certain values of chamber through-flow induce flow patterns within the chamber that are dominated by vortices. This flow pattern increases the effluent residence time in the chamber as well as the mixing of gas/particulate from the test article with air. The test article effluent jet feeds effluent into this vortical motion, and only that flow that is trapped near the chamber floor is drawn out of the chamber. Pockets of high effluent concentration can form in the chamber.

## 2. GOVERNING EQUATIONS

For purposes of producing a timely initial investigation, the cylindrical test chamber was modeled as two-dimensional (2D). The governing equations are written in Cartesian coordinates with velocity components  $u$  and  $v$  for the  $x$  (along chamber floor) and  $y$  (along chamber height) directions, respectively (see Figure 1). The Reynolds-Averaged Navier-Stokes (RANS) equations describe the 2D reacting gas flow ( $N$  species mixture) in the chamber given conditions at the boundaries of the geometry. These partial differential equations describe the time ( $t$ ) evolution of the dependent variables of velocity ( $u, v$ ), pressure

(p), mixture density ( $\rho$ ), species mass fraction ( $\sigma_i$ , for  $i = 1$  to  $N$  species), internal energy (e), temperature (T, derived from energy), and viscous shear stresses ( $\tau$ ).

$$\frac{\partial W}{\partial t} + \frac{\partial (F_1 - G_1)}{\partial x} + \frac{\partial (F_2 - G_2)}{\partial y} = \Omega. \quad (1)$$

$$W = [e, \rho, \rho u, \rho v, \rho \sigma_1, \dots, \rho \sigma_{N-1}].$$

$$F_1 = [(e+p) u, \rho u, \rho u^2 + p, \rho uv, \rho u \sigma_1, \dots, \rho u \sigma_{N-1}].$$

$$F_2 = [(e+p) v, \rho v, \rho vu, \rho v^2 + p, \rho v \sigma_1, \dots, \rho v \sigma_{N-1}].$$

$$\Omega = [0, 0, 0, 0, \sum_k \omega_{1k}, \dots, \sum_k \omega_{(N-1)k}].$$

$$G_1 = \left[ \kappa_m \frac{\partial T}{\partial x} + \sum_i \rho D (h_i - h_N) \frac{\partial \sigma_i}{\partial x} + u \tau_{xx} + v \tau_{xy}, 0, \tau_{xx}, \tau_{xy}, \rho D \frac{\partial \sigma_1}{\partial x}, \dots, \rho D \frac{\partial \sigma_{N-1}}{\partial x} \right].$$

$$G_2 = \left[ \kappa_m \frac{\partial T}{\partial y} + \sum_i \rho D (h_i - h_N) \frac{\partial \sigma_i}{\partial y} + u \tau_{yx} + v \tau_{yy}, 0, \tau_{yx}, \tau_{yy}, \rho D \frac{\partial \sigma_1}{\partial y}, \dots, \rho D \frac{\partial \sigma_{N-1}}{\partial y} \right].$$

The shear stress terms are given by

$$\tau_{xx} = 2\mu_m \frac{\partial u}{\partial x} - \frac{2\mu_m}{3} \left( \frac{\partial u}{\partial x} + \frac{\partial v}{\partial y} \right), \tau_{yy} = 2\mu_m \frac{\partial v}{\partial y} - \frac{2\mu_m}{3} \left( \frac{\partial u}{\partial x} + \frac{\partial v}{\partial y} \right), \tau_{yx} = \mu_m \left( \frac{\partial u}{\partial y} + \frac{\partial v}{\partial x} \right).$$

In these equations,  $\sigma_i$  and  $\omega_i$  are the mass fraction and chemical production terms for the  $i^{\text{th}}$  species. For the present application, finite-rate chemical production terms were not used. Chemical reaction was modeled as an infinitely fast, one-step, unidirectional (i.e., forward) reaction of smoke pot effluent ( $i = 1$ ) and air ( $i = 2$ ) to form product ( $i = 3$ ) for stoichiometric air/effluent ratio of 0.17 and effluent density above  $50 \text{ g/m}^3$ . The reaction temperature was taken as  $680^\circ \text{ C}$ .

Effluent + Air  $\rightarrow$  Product

$$\frac{\omega_1}{M_1} = -k_f \frac{\rho \sigma_1}{M_1} \frac{\rho \sigma_2}{M_2}, \quad \frac{\omega_2}{M_2} = -k_f \frac{\rho \sigma_1}{M_1} \frac{\rho \sigma_2}{M_2}, \quad \frac{\omega_3}{M_3} = +k_f \frac{\rho \sigma_1}{M_1} \frac{\rho \sigma_2}{M_2}.$$

$$k_f = 1 \times 10^{20}.$$

The temperature dependence of the species viscosity,  $\mu_i$ , and thermal conductivity,  $\kappa_i$ , can be modeled using Sutherland's law (White 1974),

$$\frac{\mu_i}{\mu_{oi}} = \left( \frac{T}{T_{op}} \right)^{3/2} \frac{T_{op} + S_\mu}{T + S_\mu}, \quad \frac{\kappa_i}{\kappa_{oi}} = \left( \frac{T}{T_{ok}} \right)^{3/2} \frac{T_{ok} + S_\kappa}{T + S_\kappa}.$$

The terms  $\mu_o$ ,  $T_o$ , and  $S$  can vary with species but were assumed to be constant with values of  $S_\mu = 199$  R,  $T_{op} = 491.6$  R,  $\mu_o = 0.1716$  mP,  $S_\kappa = 350$  R,  $T_{ok} = 491.6$  R,  $\kappa_o = 0.0139$  BTU/h-ft-R. The mixture viscosity and thermal conductivity (mixture quantities are denoted by subscript m) are determined using Wilke's law (Wilke 1950), denoting  $f$  as  $\mu$  or  $\kappa$ ,

$$f_m = \sum_i \left[ X_i f_i \left( \sum_j X_j \phi_{ij} \right)^{-1} \right], \quad \phi_{ij} = \frac{1}{\sqrt{8}} \left( 1 + \frac{M_i}{M_j} \right)^{-1/2} \left[ 1 + \left( \frac{f_i}{f_j} \right)^{1/2} \left( \frac{M_j}{M_i} \right)^{1/4} \right]^2,$$

where  $X_i$  and  $M_i$  are the mole fraction ( $X_i = \rho \sigma_i / M_i$ ) and molecular weight of the  $i^{\text{th}}$  species, respectively ( $M_1 = 97.94$ ,  $M_2 = 28.8$ , and  $M_3 = 63.37$  g/mole). Fick's law (White 1974) is used to relate the mixture diffusivity to the mixture viscosity through the Schmidt number,  $Sc = \mu_m / (\rho D)$ , assumed unity. The specific heat at constant pressure of each species (per mass) is generally given by the following fourth-order polynomial curve fit (Drummond, Rogers, and Hussaini 1987):

$$\frac{c_{p_i}}{R_i} = A_i + B_i T + C_i T^2 + D_i T^3 + E_i T^4.$$

For the present study,  $c_p$  was assumed constant with values  $c_{p1} = 0.2878$ ,  $c_{p2} = 0.238$ , and  $c_{p3} = 0.1277$  cal/g°C. The mixture pressure (equation of state), enthalpy, total energy per unit volume,

and ratio of specific heats are given by ( $R_u$  is the universal gas constant and  $\Delta H_f$  is the heat of formation for species  $i$ )

$$p = \sum_i p_i = \rho T R_u \sum_i \frac{\sigma_i}{M_i} ,$$

$$h = \sum_i \sigma_i \int^T c_{p_i} dT + \sum_i \sigma_i \Delta H_{f_i} ,$$

$$e = \frac{p}{\gamma-1} + \rho \frac{(u^2 + v^2)}{2} + \sum_i \rho \sigma_i \Delta H_{f_i} ,$$

$$\gamma = 1 + \left[ \frac{c_{p_m}}{R_u \sum_i (\sigma_i / M_i)} - 1 \right]^{-1} ,$$

and

$$c_{p_m} = \frac{1}{T} \sum_i \sigma_i \int^T c_{p_i} dT .$$

An algebraic turbulence model (Bradshaw, Cebeci, and Whitelaw 1981) was used. In this model, the eddy viscosity,  $\mu_t$ , is computed assuming that the viscous layer consists of an inner and an outer component. The inner region follows the Prandtl mixing length formulation based on a prescribed characteristic length scale,  $L$ , a boundary layer intermittency factor,  $\epsilon$  (having a value of 0 for laminar, 1 for turbulent flows, and a function of  $x$  for transitional flows), the displacement thickness of the layer,  $\delta$ , and a constant,  $a$ .

$$(\mu_t)_{\text{inner}} = L^2 y \left\| \frac{\partial u}{\partial y} \right\| , \quad 0 \leq y \leq y_c .$$

$$(\mu_t)_{\text{outer}} = a u_e \left\| \delta \right\| \epsilon , \quad y_c \leq y \leq y_e .$$

Here,  $y_c$ , is a prescribed, small distance from the solid boundary, and  $y_e$  is the edge of the viscous layer. Further details can be obtained from Bradshaw, Cebeci, and Whitelaw (1981). The fluid viscosity is then  $\mu = \mu_m(T) + \mu_v$ , where  $\mu_m(T)$  is obtained using Sutherland's law and Wilke's law.

### 3. BOUNDARY CONDITIONS AND INITIAL CONDITIONS

The boundaries of the test chamber (see Figure 1) are the air inlet at the top (roof), the exit port on the chamber floor (connected by ducts to the wind tunnel fan), and the vertical walls. The smoke pot is placed on the chamber floor, near the chamber exit port. Since the governing equations are elliptic (low-speed flow), conditions along these boundaries must prescribe values of the dependent variables, the gradient of the dependent variables in the boundary-normal direction, or an algebraic relation which connects the values of the dependent variables to the normal component of velocity.

At the air inlet, x-direction profiles of all dependent variables,  $p$ ,  $u$ ,  $v$ ,  $\sigma$ ,  $T$ , and  $\rho$ , are specified. It is assumed that the flow at the inlet consists of air and that convection/diffusion of effluent to the chamber top is not permitted to exit the chamber. By mass conservation, the inlet flow velocity was specified as  $u = .062$  ft/s, and a parabolic-shaped profile was assumed.

The exit port velocity was specified as  $u = 2.96$  ft/s (5,380 l/min) with a parabolic-shaped profile. Boundary-normal gradients of all dependent variables at the exit plane are zero. Mass that exits the port is not assumed to reenter.

The no-slip/no-penetration condition ( $u = v = 0$ ) is applied to the solid chamber and smoke pot walls. The walls are assumed to be adiabatic (i.e., normal derivative of  $T$  set to zero). The normal gradient of all mass fractions,  $\partial\sigma_i/\partial n$ , are also set to zero.

The top of the smoke pot was assumed to be a constant mass flux source of effluent with  $u = 12.7$  ft/s,  $T = 320^\circ$  C,  $M_1 = 97.94$  g/mole, and  $c_p = 0.2878$  cal/g $^\circ$  C.

### 4. COMPUTATIONAL ALGORITHM

Equation (1) can be reduced to a successive-substitution formula for a general dependent variable,  $W$ , at each node on the computational grid. Central finite-differences are used for the diffusive (arrays  $G_1$

and  $G_2$ ) and source terms (array  $\Omega$ ) and upwind differences for the convective terms (arrays  $F_1$  and  $F_2$ ). Using upwind differencing in the species conservation equations (i.e.,  $W = \rho\sigma_i$ ) reduces the occurrence of negative species mass fractions in mixing layers. The resulting system of equations for the entire grid is solved using a Gauss-Seidel relaxation scheme. Each iteration cycle is made up of  $J$  subcycles, where  $J$  is the number of equations being considered. In each subcycle, grid points are scanned row by row, and a single variable is updated. When all subcycles are completed, a new iteration cycle in which the values of the variables from the latest iteration are immediately used is started. This is consistent with the Gauss-Seidel methodology. Convergence is satisfied when the greatest relative change in any flow variable is smaller than a prescribed tolerance. See Nusca (1989, 1991) for further details.

## 5. RESULTS AND DISCUSSION

Figure 1 shows the computational grid used to discretize the chamber interior. The number of grid nodes in the  $x$  and  $y$  directions are 75 and 50, respectively (3,750 nodes total). Grid node clustering was used to resolve flow gradients near the smoke pot.

The simulation was run for approximately 1 min to establish steady flow in the chamber before the smoke pot was activated. Figure 2 shows the streamline (contour lines of constant stream function) patterns. Note that a large counterclockwise vortex resides to the upper left of the smoke pot (established by flow from the chamber inlet that must turn at the chamber floor) and that a smaller clockwise vortex resides over the smoke pot (established by flow rising in the vertical direction that is turned by the chamber inlet flow at the top).

Figures 3, 4, 5, and 6 show the flow streamline pattern after 1, 2, 3, and 4 min of smoke pot operation, respectively. Initially, flow from the smoke pot rises toward the chamber top, establishing two small vortices near the pot, rotating in opposite directions. At later times, the flow settles into a large counterclockwise vortex offset from the centerline of the chamber and fed by the smoke pot jet. Flow entrained in the chamber exit port is limited to that trapped near the chamber floor. Figure 7 shows the flow streamline pattern at 4.5 min, which is 0.5 min after the smoke pot has ceased operation. The vortex has reduced in size and is centered between the vertical chamber walls.

Figures 8–12 and Figures 13–17 show contours of smoke pot effluent mass fraction,  $\sigma_1$ , (mass of effluent/total mass) and effluent density (product of mass fraction and mixture density), respectively, at



times 1–4.5 min. At early times, effluent concentrations are high in the smoke pot jet. At later times, the effluent is entrained in the chamber vortex and diffused to smaller concentrations. Even at later times, pockets of high concentration ( $50 \text{ g/m}^3$  or greater) can be noted. The flow pattern is not greatly disturbed by the chamber exit port on the floor. Figures 12 and 17 show the effluent mass fraction and density at 4.5 min, 0.5 min after flow from the smoke pot has been stopped. The chamber vortex has swept effluent into the vicinity of the smoke pot where it becomes trapped at large concentration levels.

## 6. CONCLUSIONS

Due to the low-vertical flow velocity (0.06–2.7 ft/s) through the chamber induced by the small chamber exit port on the floor, the natural flow pattern in the chamber is one that is dominated by rotating vortices. This pattern increases the flow residence time in the chamber and mixes gases from the smoke pot with air (similar to a "well-stirred reactor"). The smoke pot jet feeds effluent into this vortical motion, with only that flow that is trapped near the chamber floor exiting the chamber. As a result, effluent is allowed to form pockets of high concentration that may chemically react with the fresh-air supply fed from the chamber inlet (i.e., top). After the smoke pot ceases operation, the chamber vortex concentrates effluent near the chamber wall. A larger chamber exit port and forced exit velocity (controlled by the wind tunnel fan) may assist in breaking these vortices and evacuating the chamber at the higher rate. The increased chamber through-flow should be sufficient to turn the smoke pot jet toward the exit. Numerical simulations aimed at predicting this effect have not been pursued.

The numerical simulations, results, discussions, and conclusions reached in this report are subject to the assumptions used in the model and the information supplied to the model in the form of boundary conditions. While the confidence level in the model is high (based on performance in simulating other problems), further studies that test model sensitivity to the supplied boundary conditions should be conducted. A full three-dimensional simulation should be conducted to model the perforated chamber top wall, in addition to three discrete smoke pot exit holes as well as flow obstructions (i.e., pipes) in the chamber. These are thought to represent secondary effects in the simulation of unknown final effect on the results.

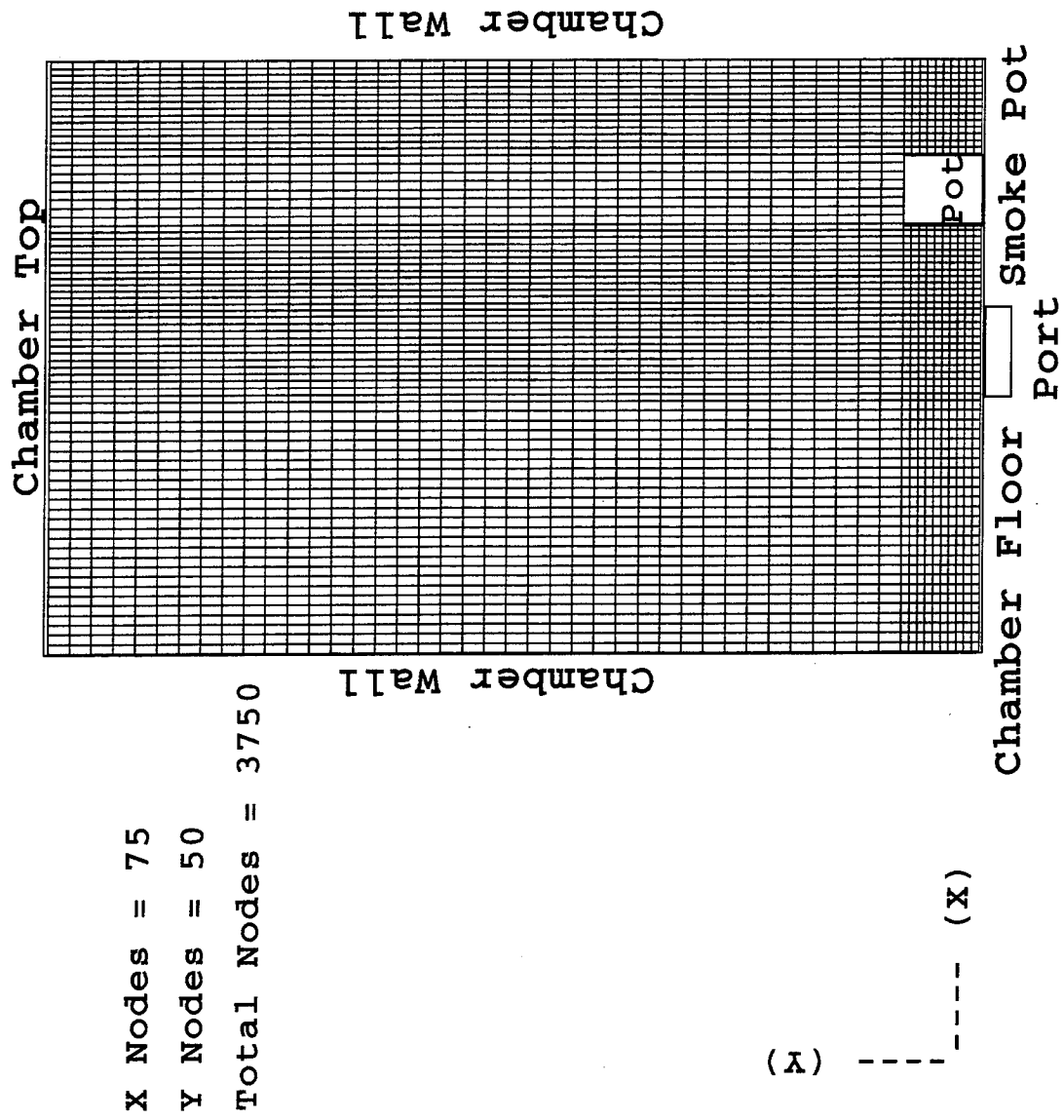


Figure 1. Schematic of test chamber and smoke pot showing computational grid.

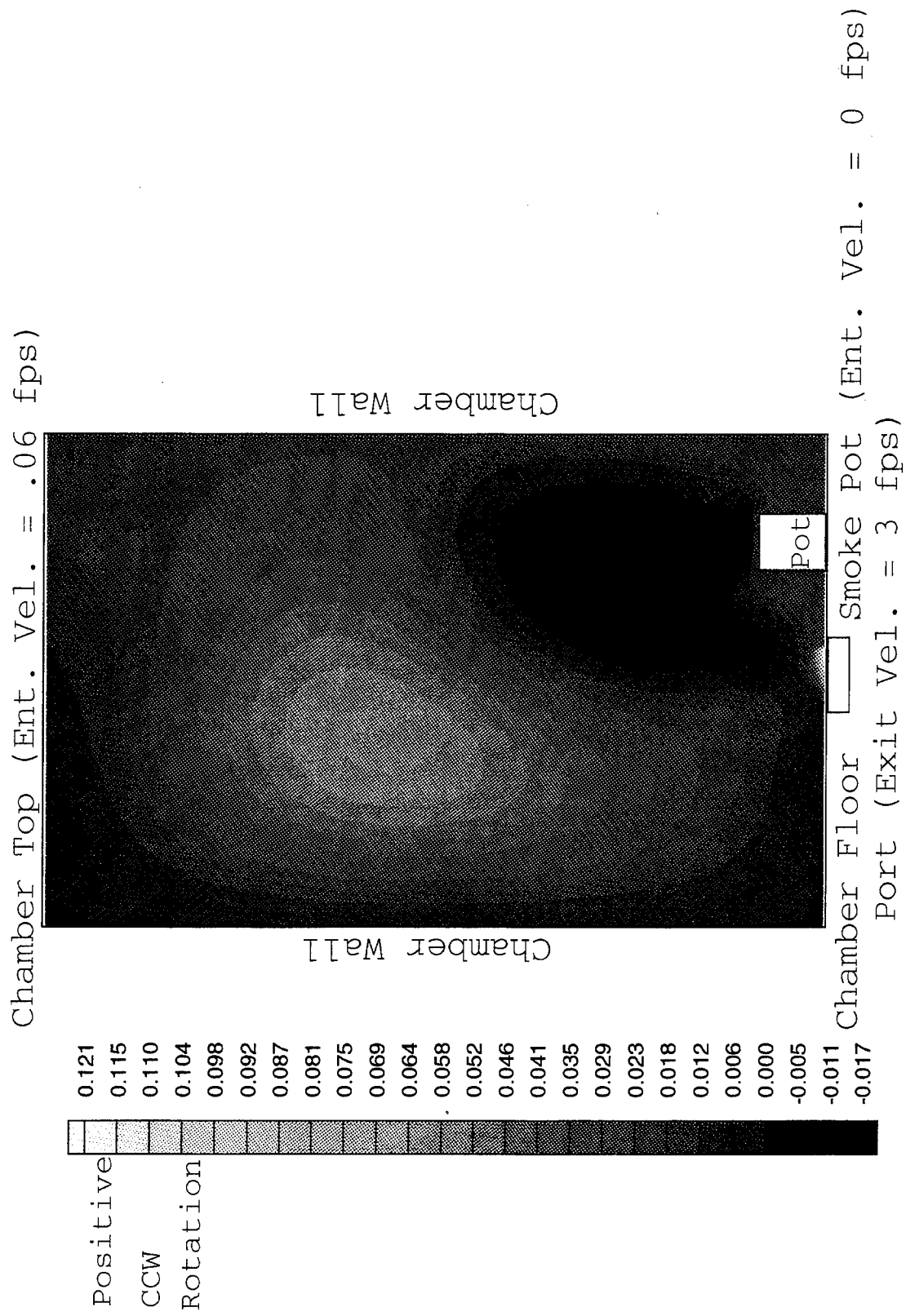


Figure 2. Stream function contours before smoke pot operation.

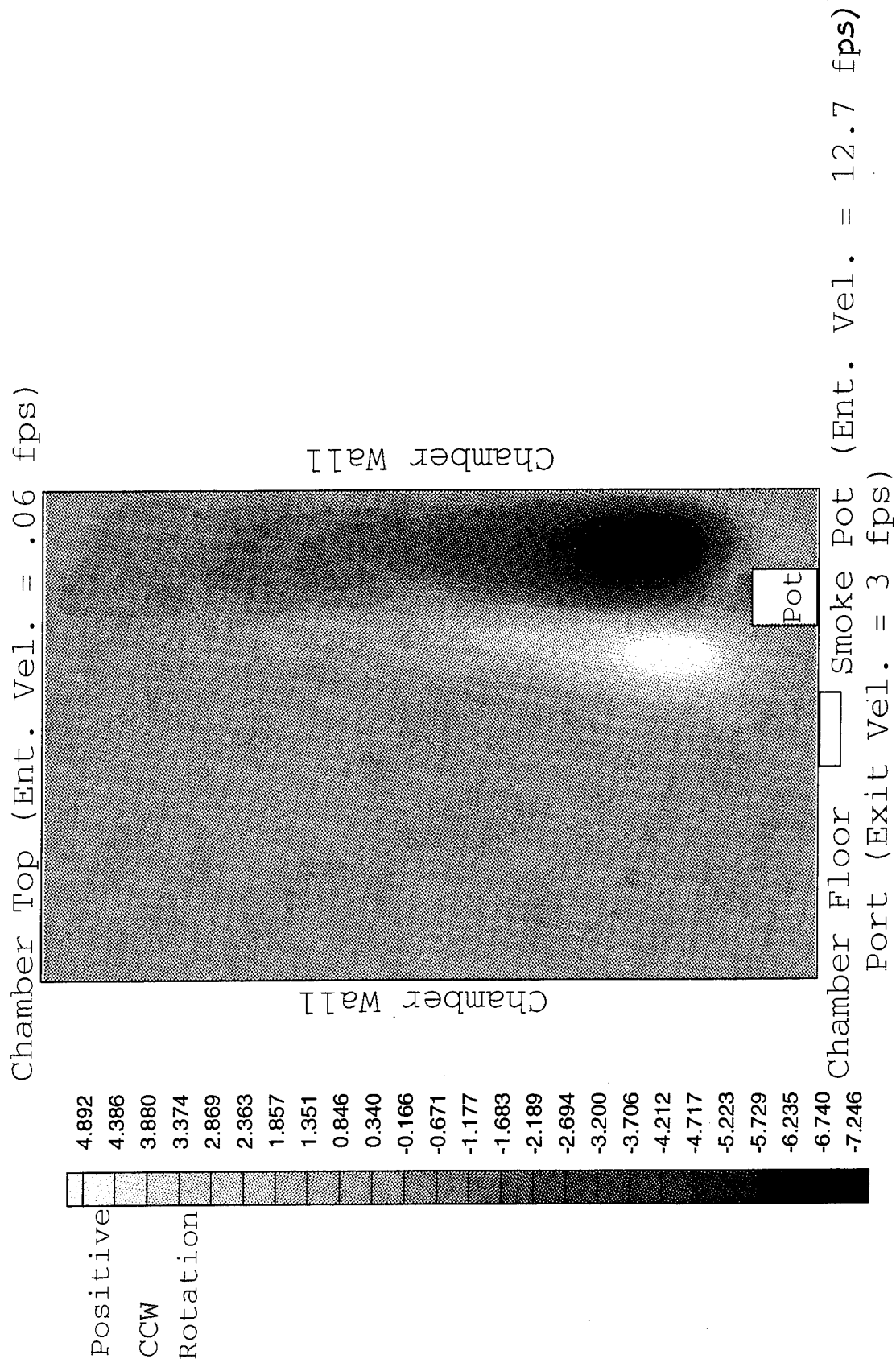


Figure 3. Stream function contours 1.0 min after smoke pot startup.

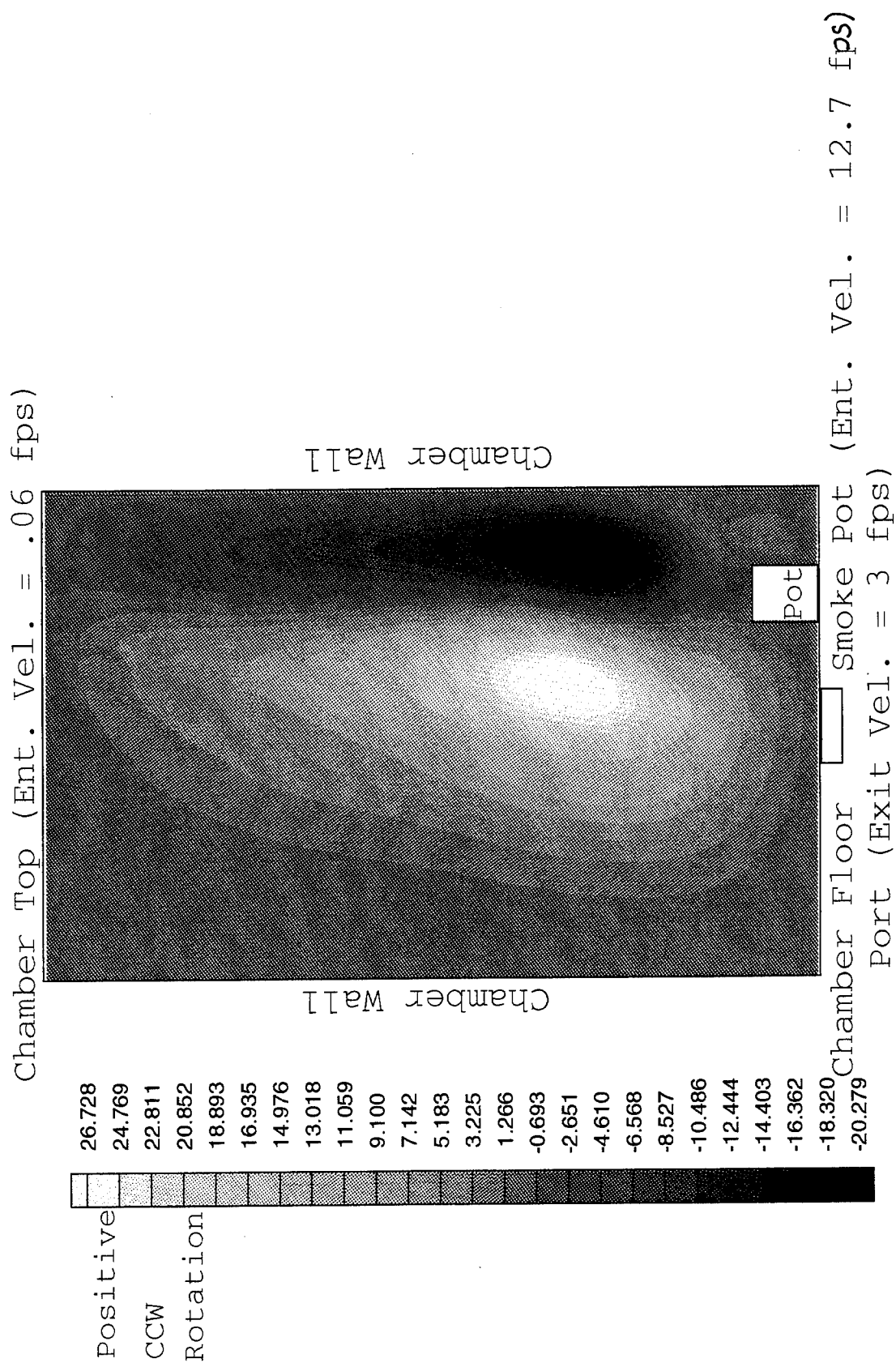


Figure 4. Stream function contours 2.0 min after smoke pot startup.

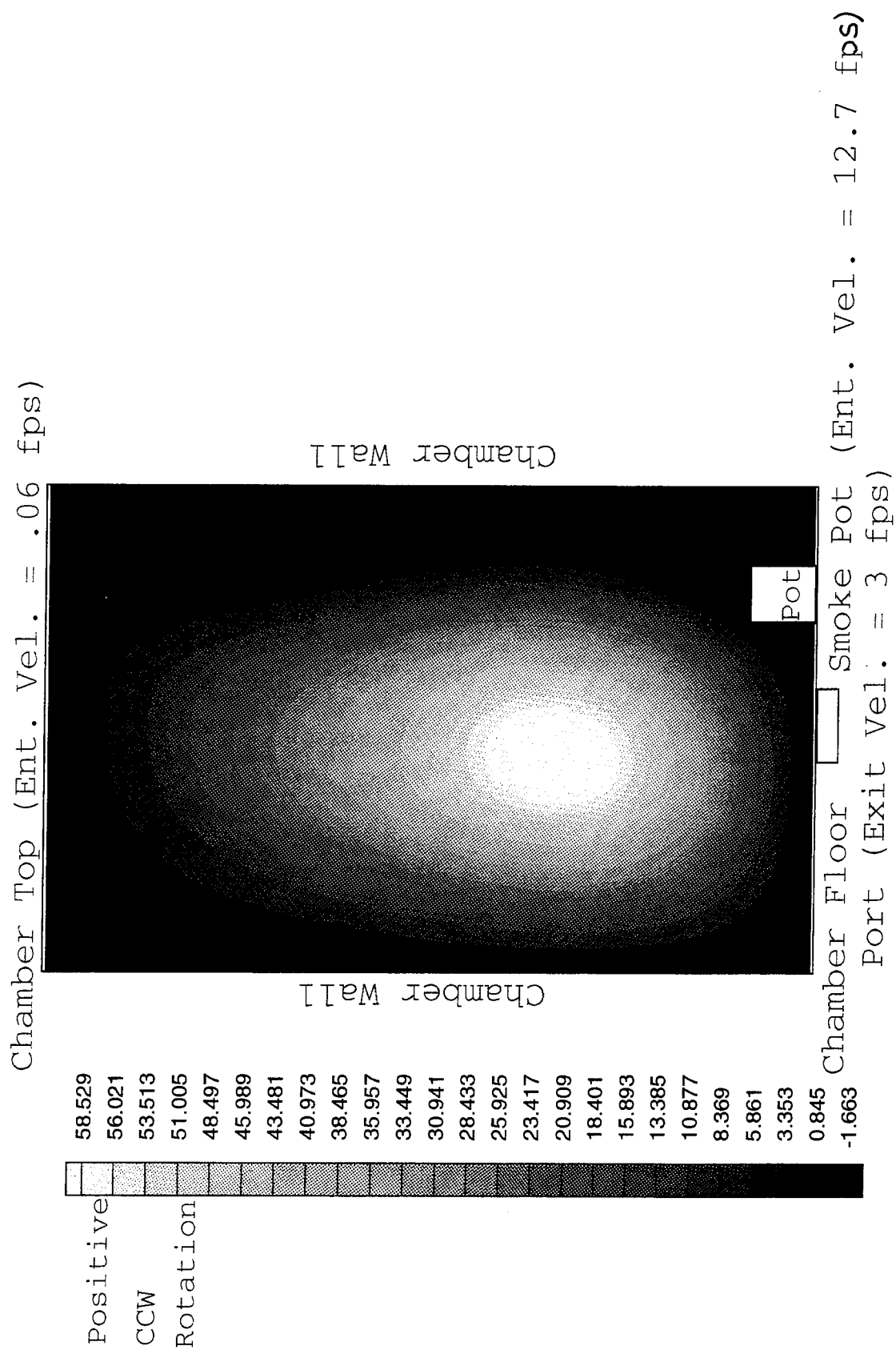


Figure 5. Stream function contours 3.0 min after smoke pot startup.

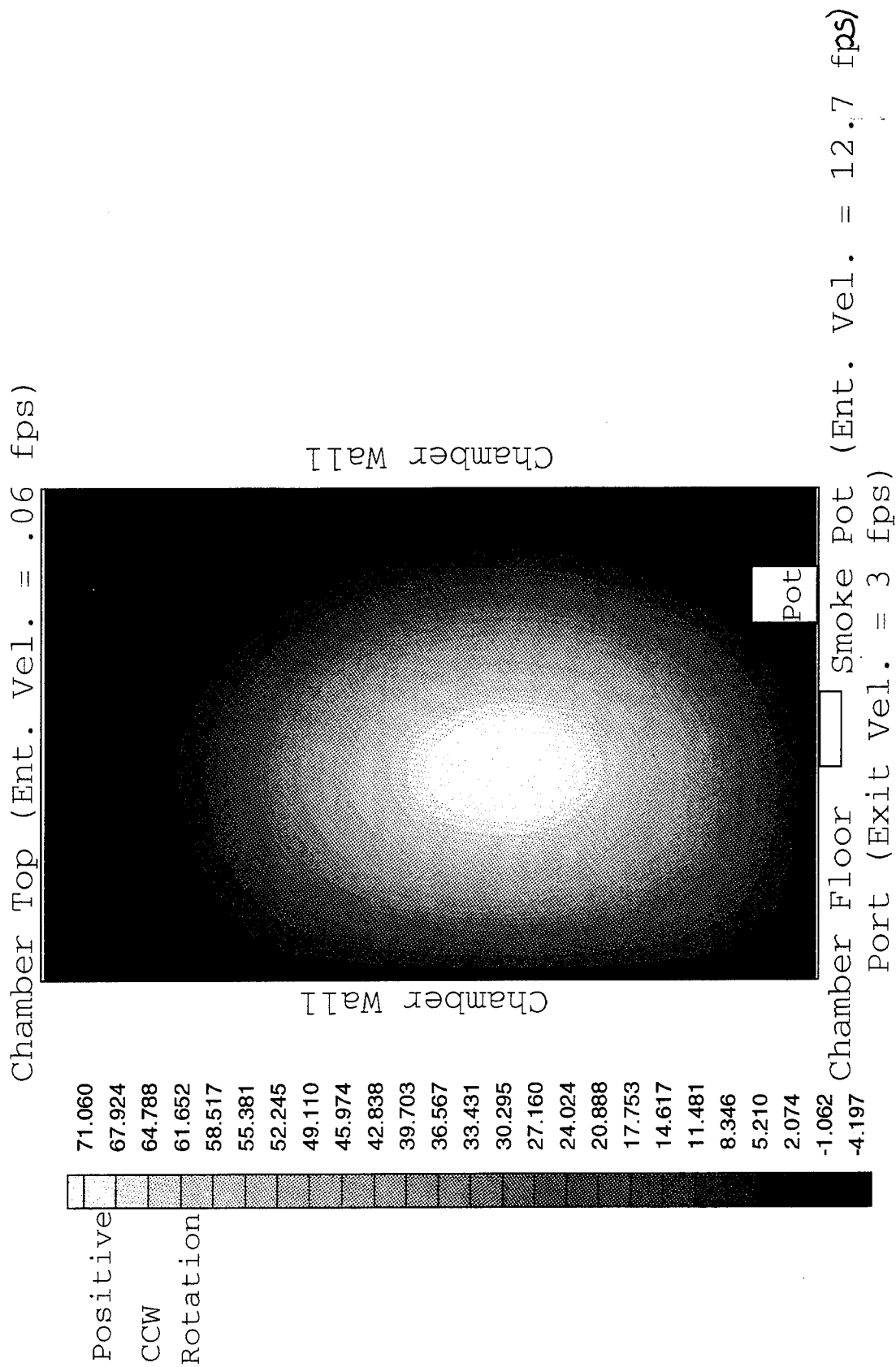


Figure 6. Stream function contours 4.0 min after smoke pot startup.

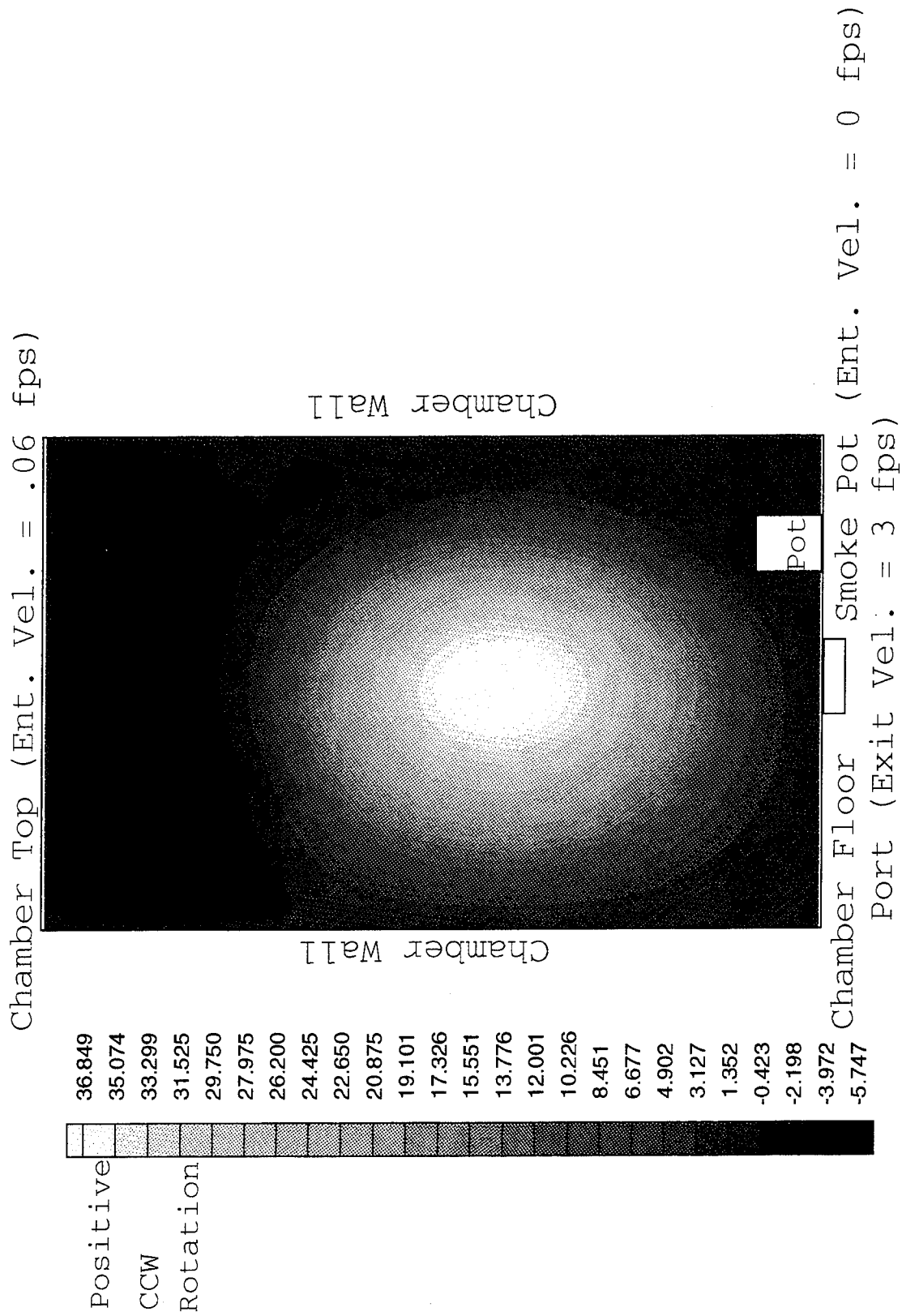


Figure 7. Stream function contours 4.5 min after smoke pot startup, 0.5 min after smoke pot termination.



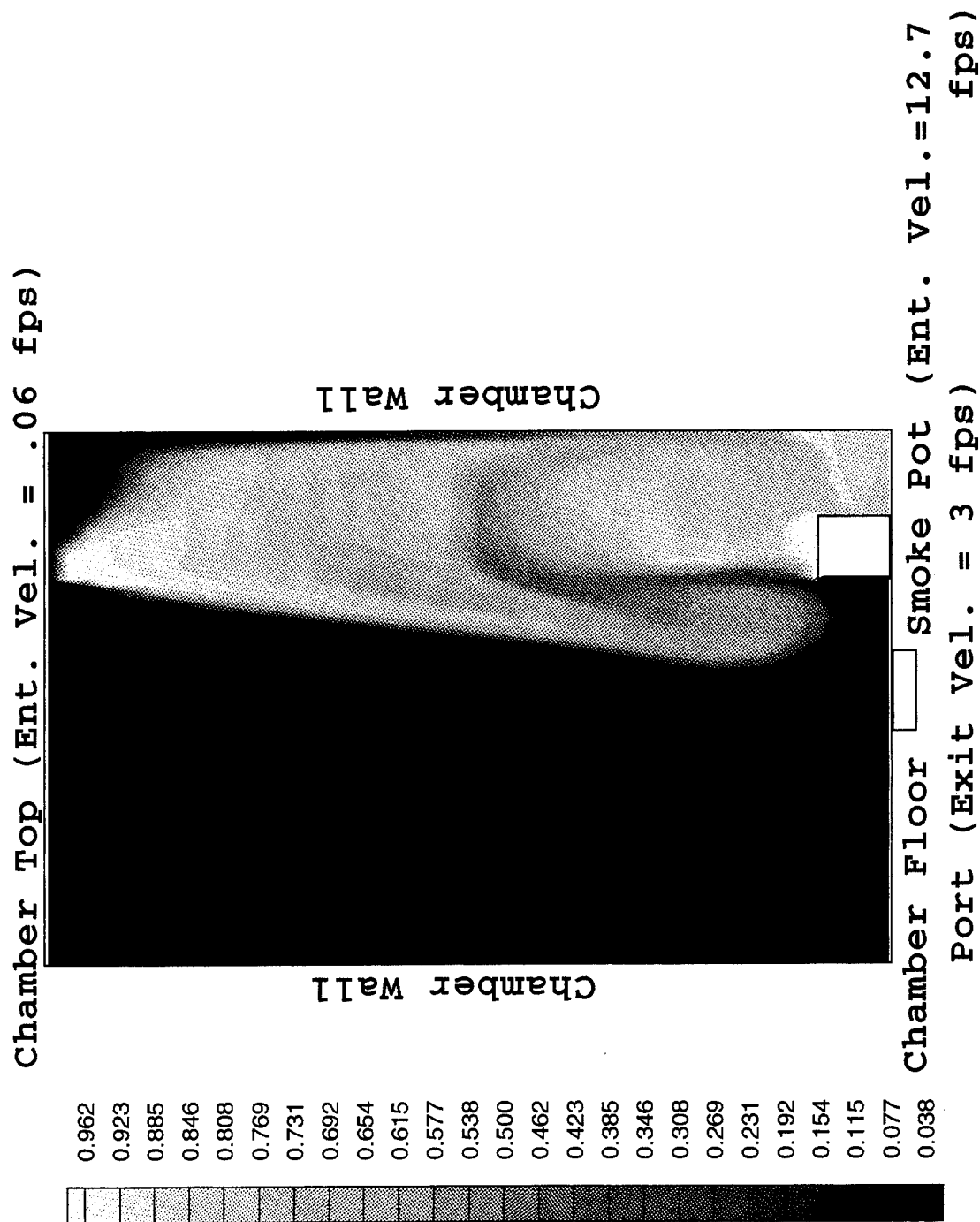


Figure 8. Effluent mass fraction contours 1.0 min after smoke pot startup.

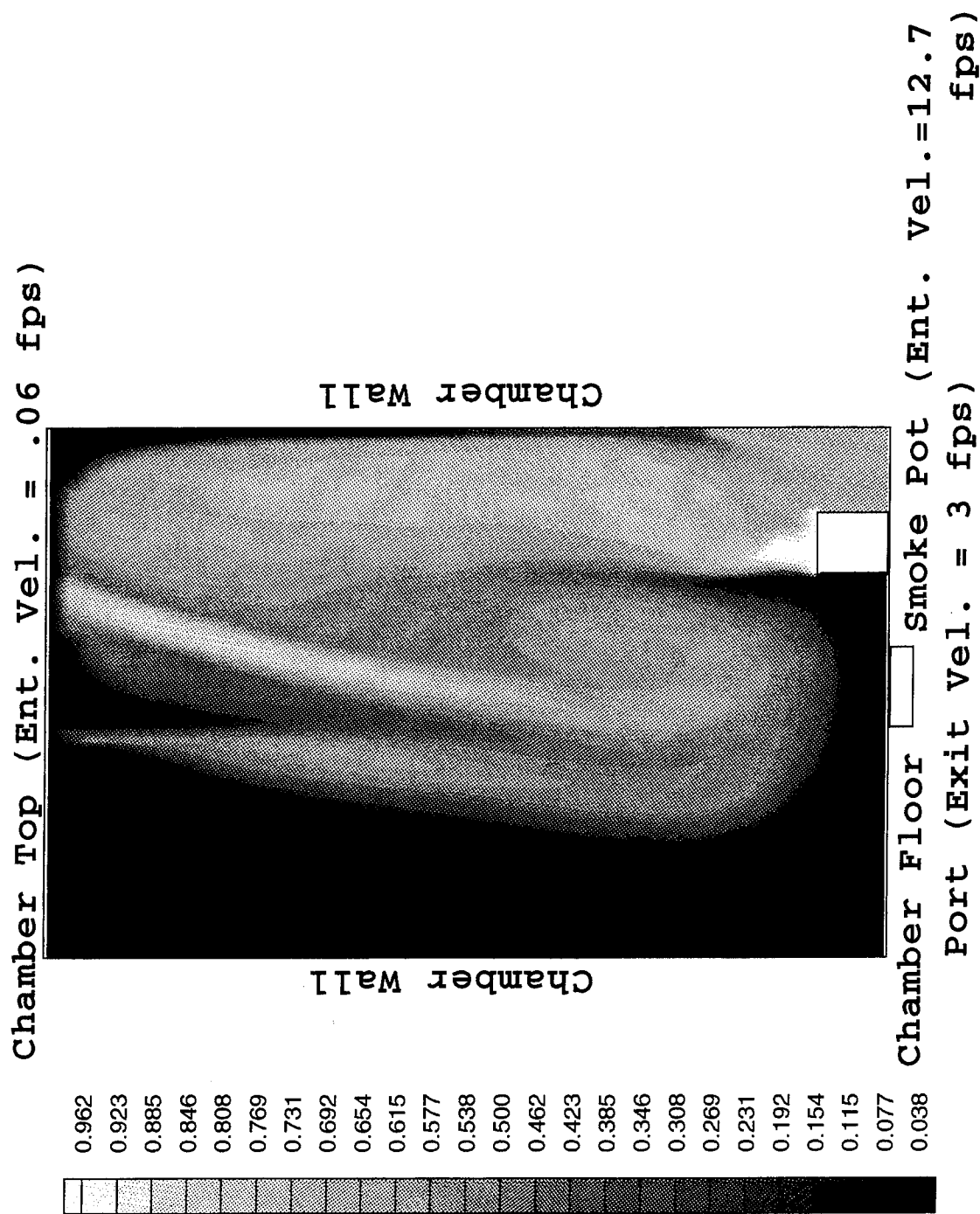


Figure 9. Effluent mass fraction contours 2.0 min after smoke pot startup.

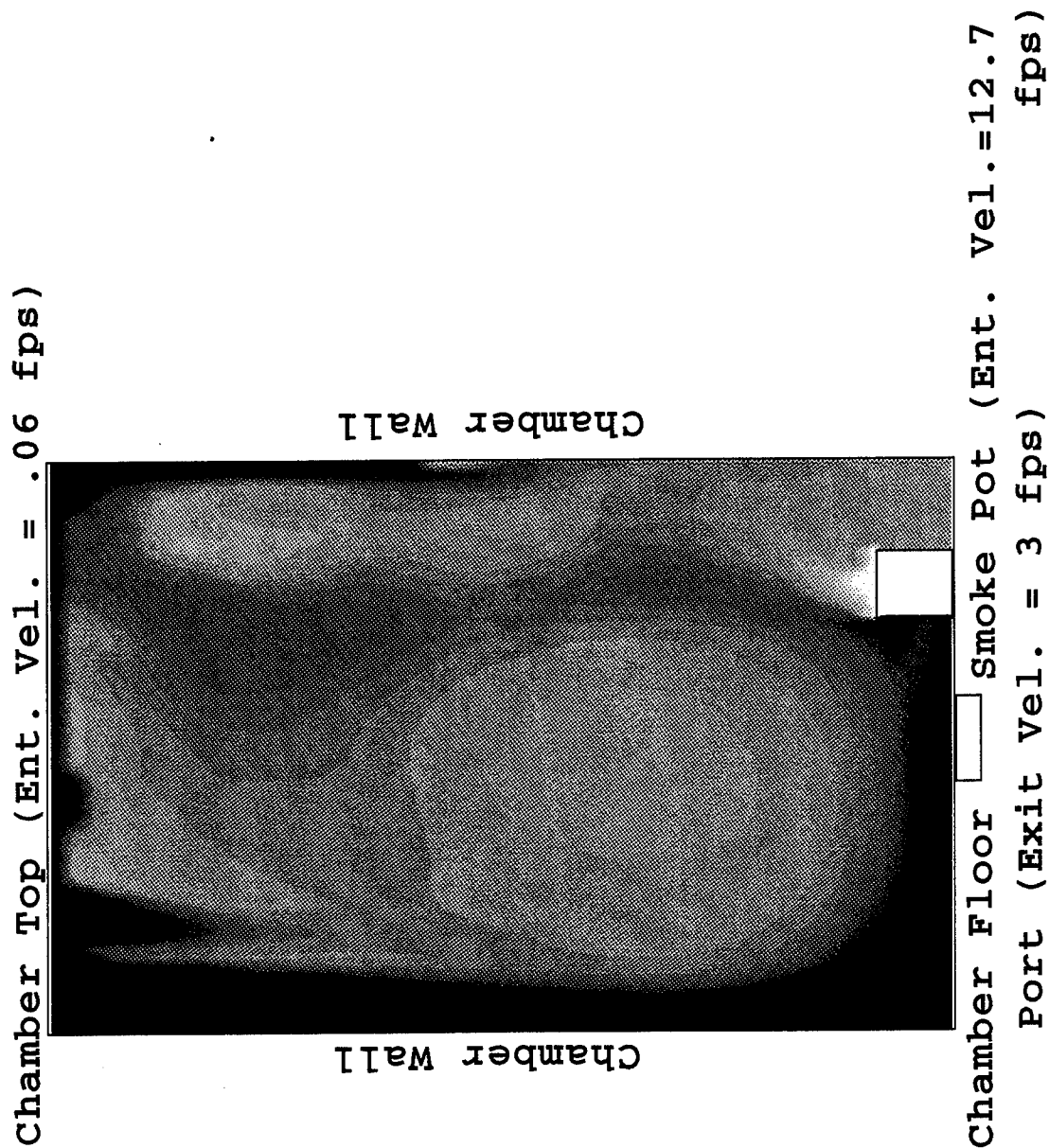


Figure 10. Effluent mass fraction contours 3.0 min after smoke pot startup.

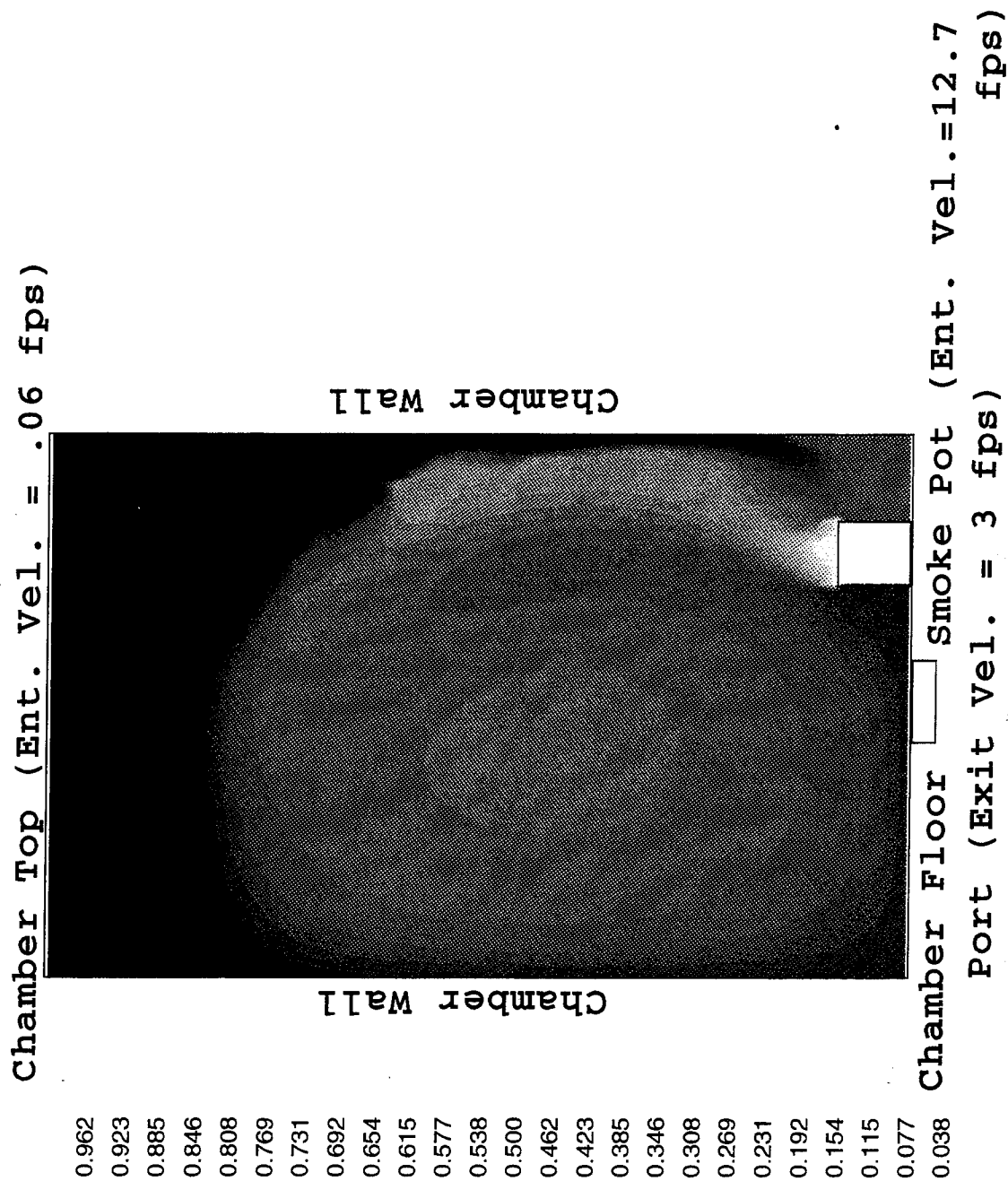


Figure 11. Effluent mass fraction contours 4.0 min after smoke pot startup.

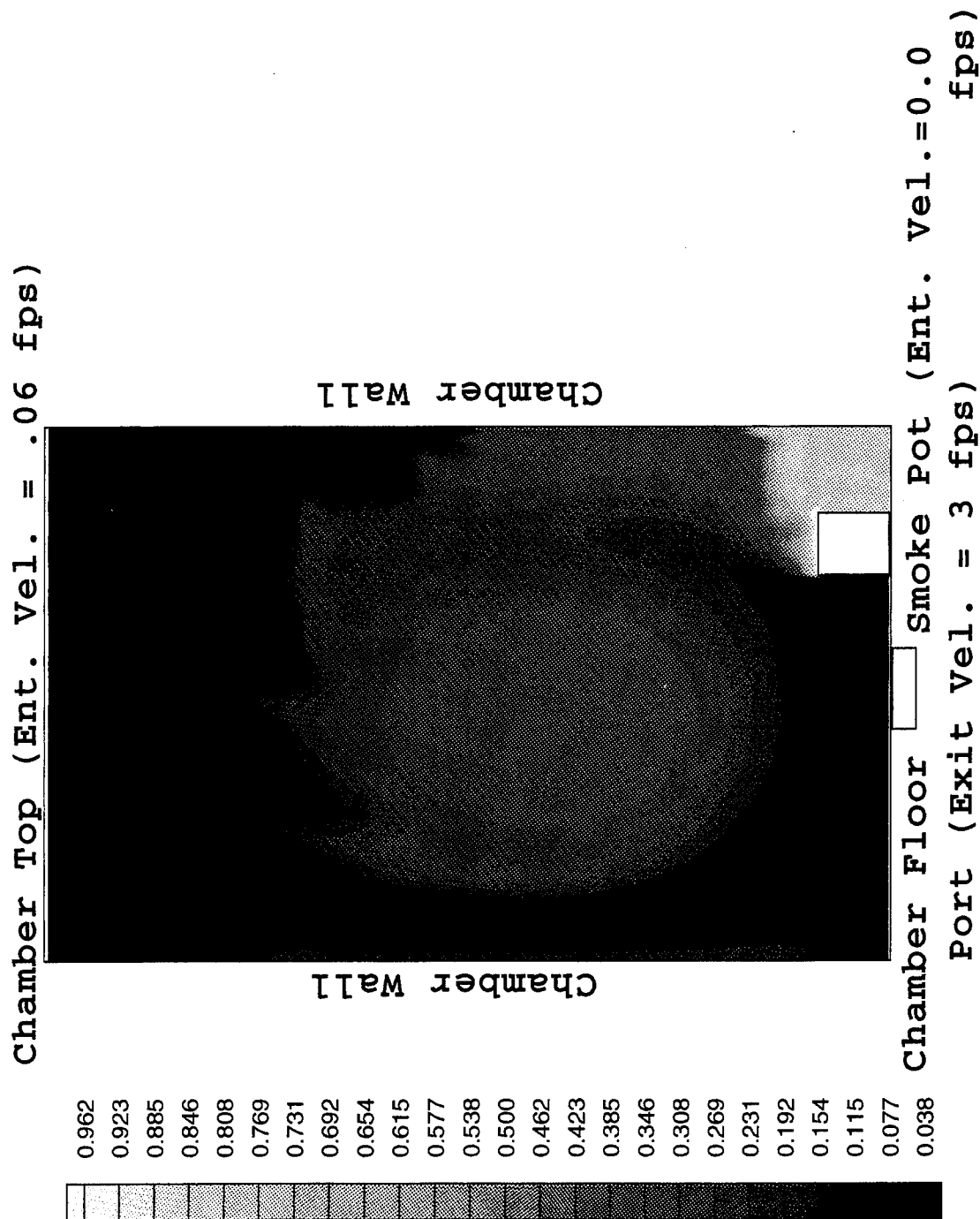


Figure 12. Effluent mass fraction contours 4.5 min after smoke pot startup, 0.5 min after smoke pot termination.

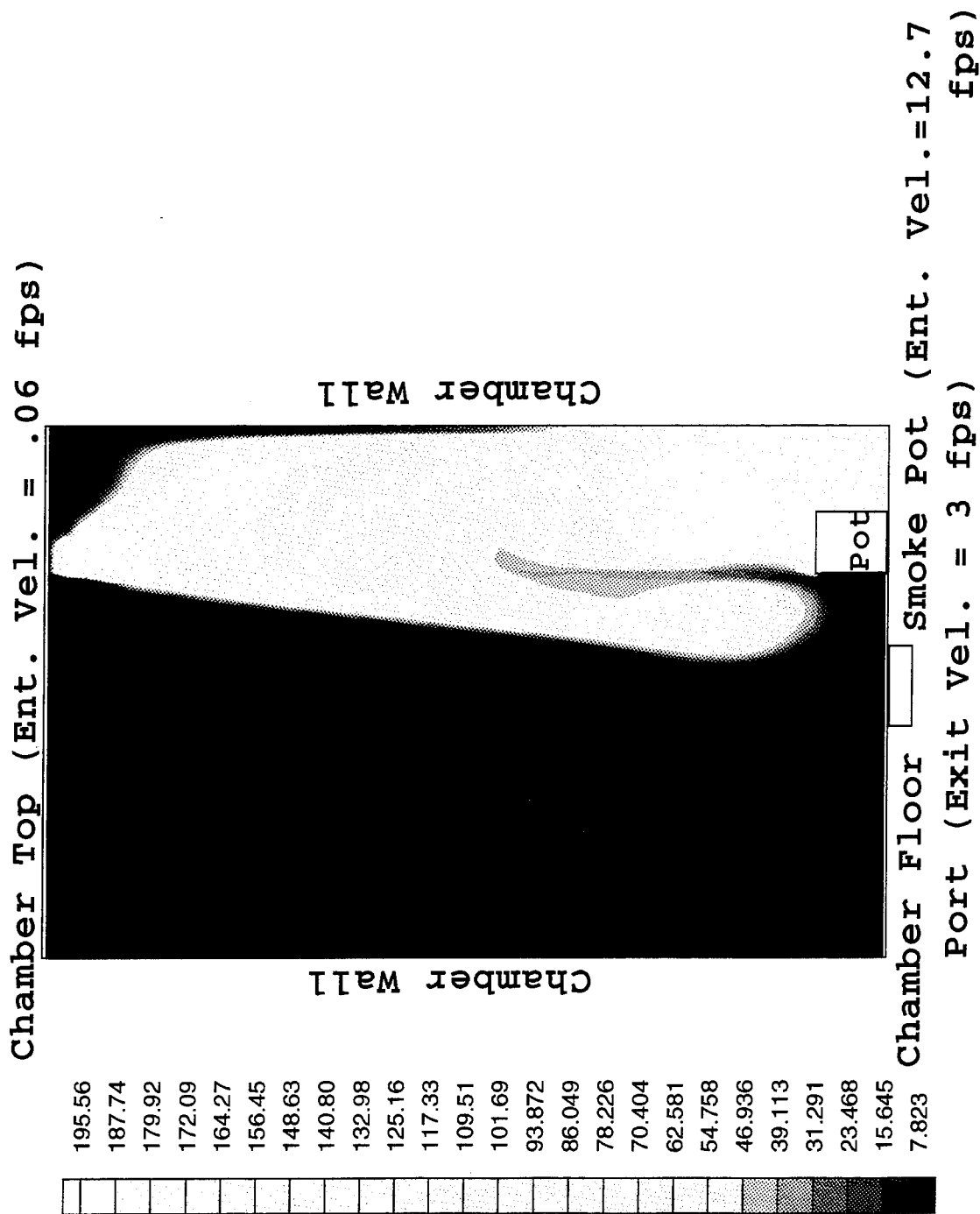


Figure 13. Effluent density ( $\text{g/m}^3$ ) contours 1.0 min after smoke pot startup.

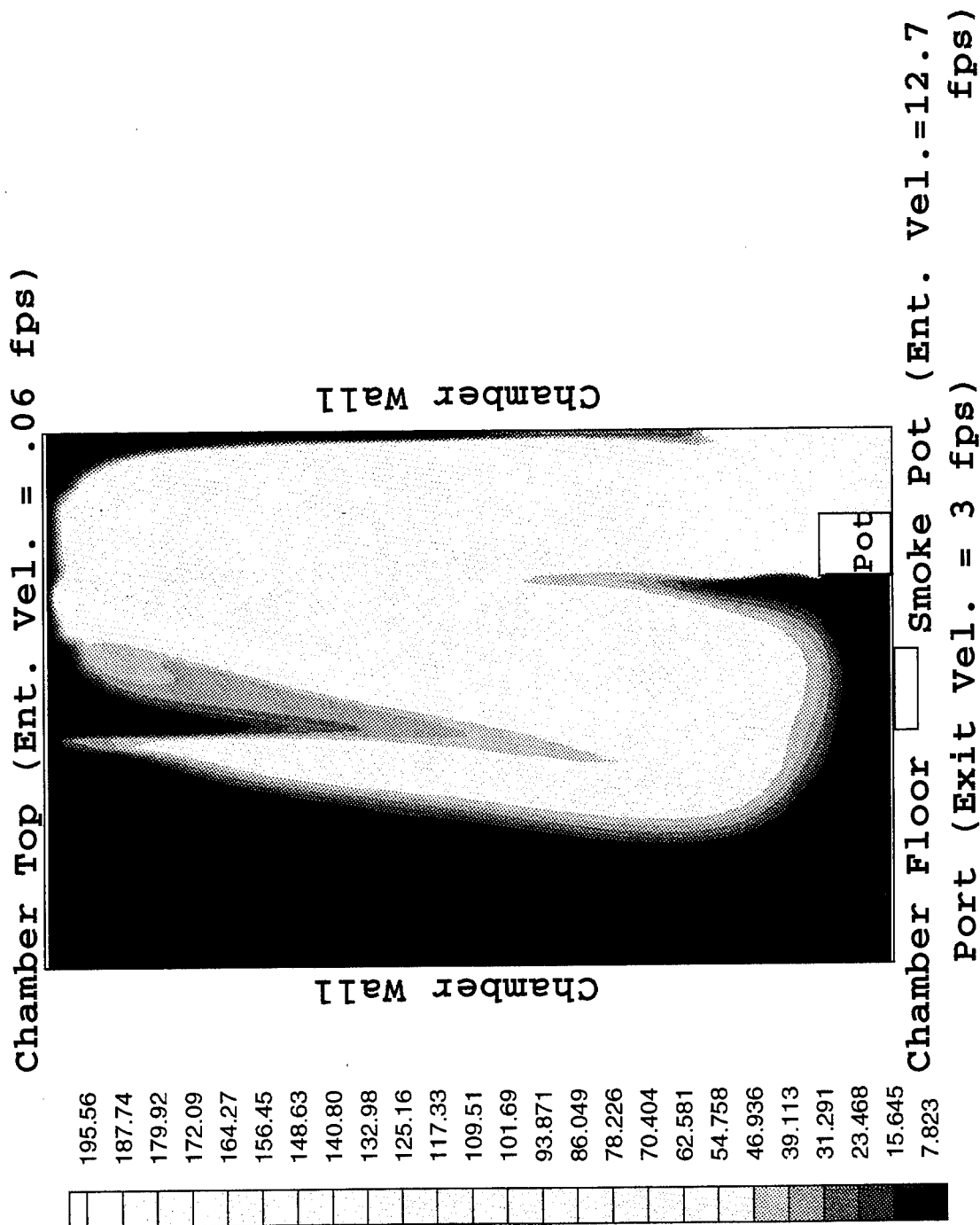


Figure 14. Effluent density ( $\text{g/m}^3$ ) contours 2.0 min after smoke pot startup.

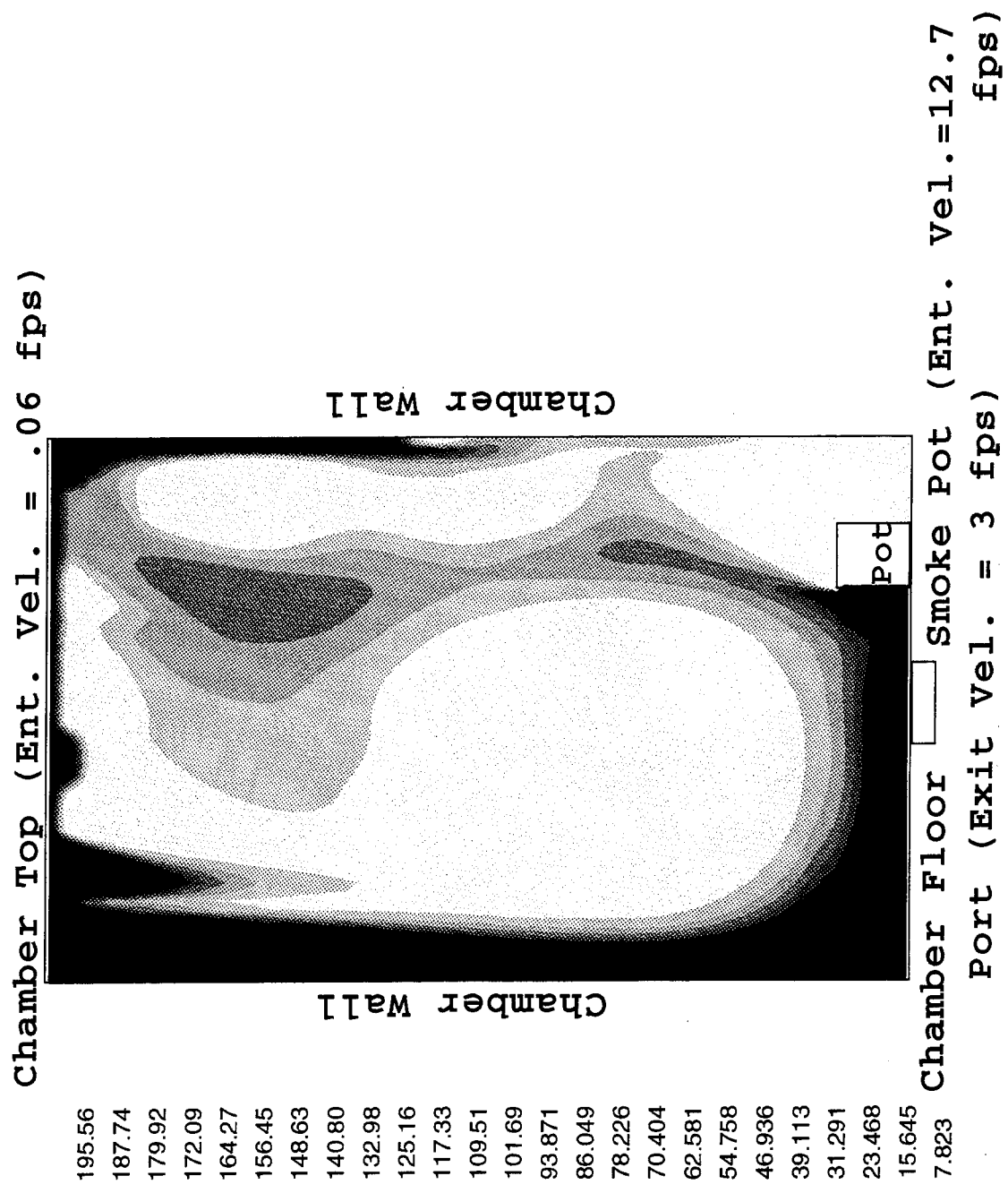


Figure 15. Effluent density ( $\text{g/m}^3$ ) contours 3.0 min after smoke pot startup.



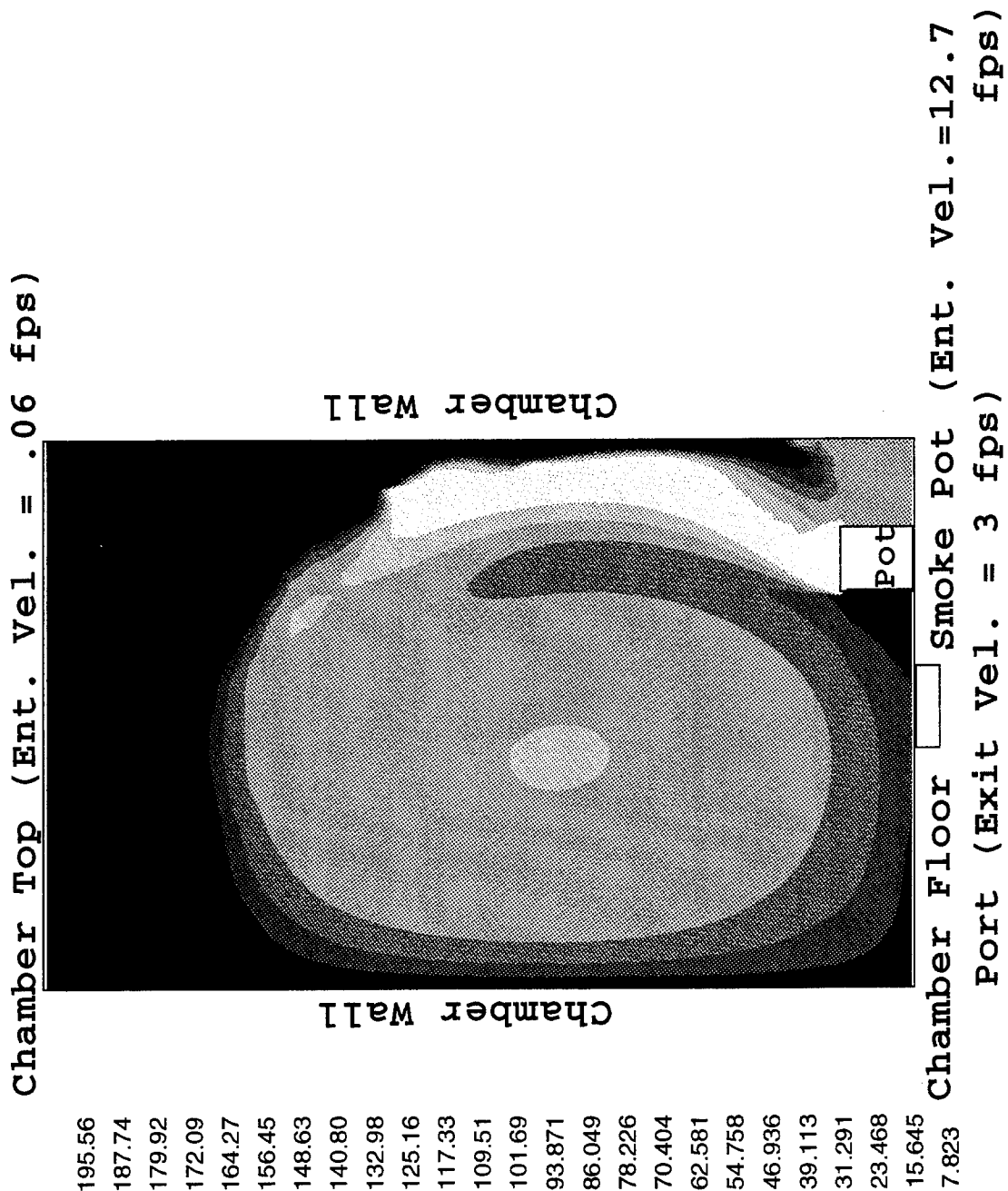


Figure 16. Effluent density ( $\text{g/m}^3$ ) contours 4.0 min after smoke pot startup.

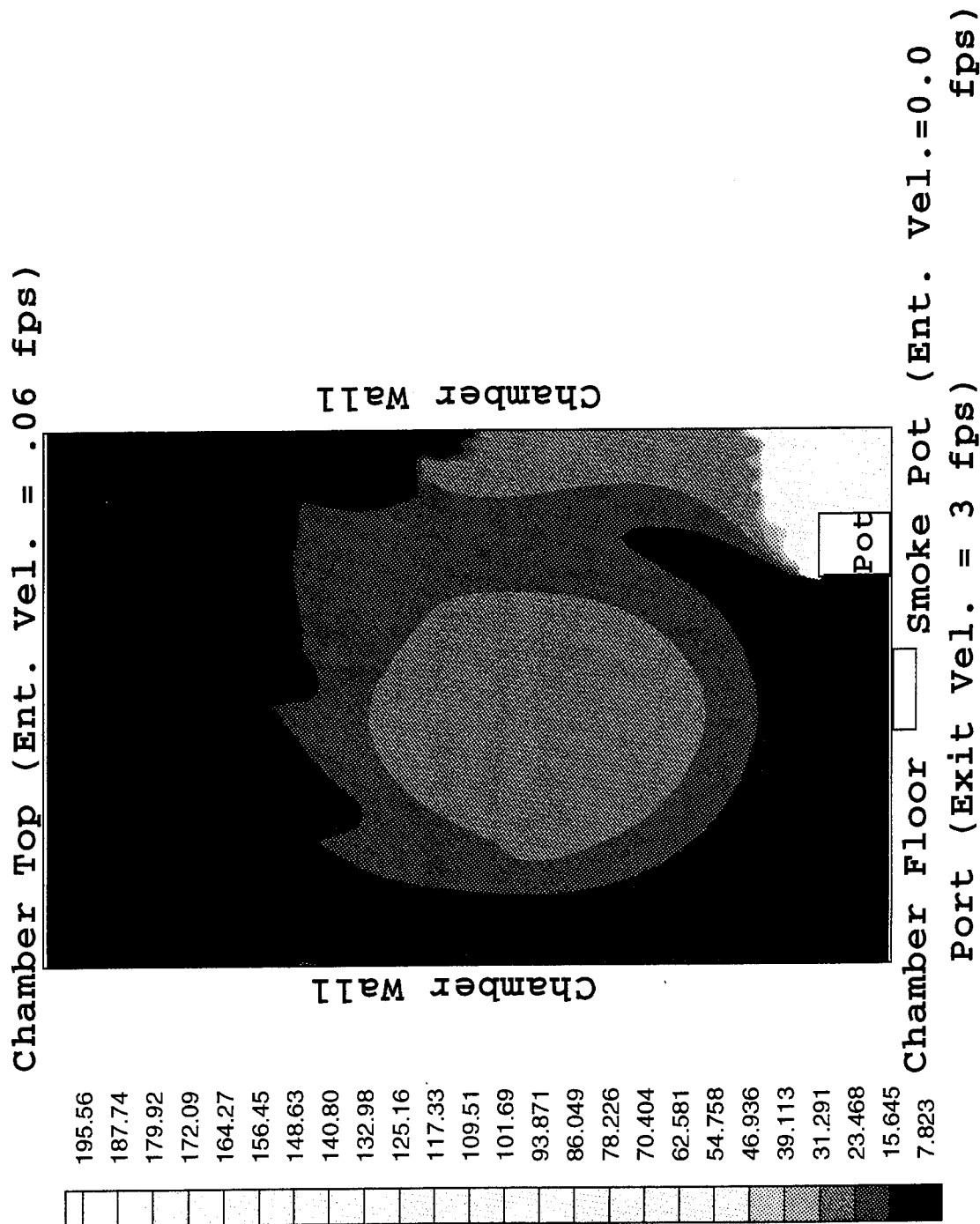


Figure 17. Effluent density ( $\text{g/m}^3$ ) contours 4.5 min after smoke pot startup, 0.5 min after smoke pot termination.

## 7. REFERENCES

- Baldwin, B. S., and H. Lomax. "Thin-Layer Approximation and Algebraic Model for Separated Turbulent Flows." AIAA Paper No. 78-257, January 1978.
- Bradshaw, P., T. Cebeci, and J. H. Whitelaw. Engineering Calculation Methods for Turbulent Flow. New York: Academic Press, 1981.
- Drummond, J. P., C. Rogers, and M. Y. Hussaini. "A Numerical Model for Supersonic-Reacting Mixing Layers." Computer Methods in Applied Mechanics and Engineering, vol. 64, 1987.
- Nusca, M. J. "Steady Flow Combustion Model for Solid-Fuel Ramjet Projectiles." BRL-TR-2987, U.S. Army Ballistic Research Laboratory, Aberdeen Proving Ground, MD, April 1989.
- Nusca, M. J. "Numerical Simulation of Reacting Flow in a Thermally Choked Ram Accelerator -- Model Development and Validation." BRL-TR-3222, U.S. Army Ballistic Research Laboratory, Aberdeen Proving Ground, MD, April 1991.
- Nusca, M. J. "Numerical Simulation of Fluid Dynamics and Payload Dissemination in a Dual-Chamber Grenade." ARL-TR-77, U.S. Army Research Laboratory, Aberdeen Proving Ground, MD, February 1993.
- White, F. M. Viscous Fluid Flow. New York: McGraw-Hill Book Co., 1974.
- Wilke, C. R. "A Viscosity Equation for Gas Mixtures." Journal of Chemistry and Physics, vol. 18, no. 4, pp. 517-519, 1950.

INTENTIONALLY LEFT BLANK.

## LIST OF SYMBOLS

$c_p$	=	specific heat capacity, constant p
$c_v$	=	specific heat capacity, constant volume
$D$	=	mass diffusion coefficient
$e$	=	specific total internal energy
$F, G$	=	flux vectors
$h$	=	molar specific enthalpy
$L$	=	Prandtl mixing length
$M$	=	molecular weight
$N$	=	total number of species
$p$	=	static pressure
$R$	=	specific gas constant, $(\gamma-1)c_p/\gamma$
$R_u$	=	universal gas constant, $R M_m$
$Sc$	=	Schmidt Number, $\mu_m/\rho D$
$t$	=	time
$T$	=	static temperature
$u$	=	axial velocity
$v$	=	radial velocity
$W$	=	dependent variable vector
$x, y$	=	Cartesian coordinates
$X$	=	species mole fraction

### Greek Symbols

$\gamma$	=	ratio of specific heats, $c_p/c_v$
$\Delta H_f$	=	enthalpy of formation
$\delta$	=	boundary layer displacement thickness
$\varepsilon$	=	boundary layer intermittency factor
$\kappa$	=	heat transfer coefficient
$\mu$	=	molecular viscosity

$\rho$	=	density
$\sigma$	=	species mass fraction
$\tau$	=	shear stress tensor
$\omega$	=	chemical production term
$\Omega$	=	source term vector

### Subscripts

e	=	edge of the viscous layer
i	=	$i^{\text{th}}$ species
m	=	mixture quantity
p	=	constant pressure
t	=	turbulence quantity
v	=	constant volume
x	=	x-direction
y	=	y-direction

<u>NO. OF COPIES</u>	<u>ORGANIZATION</u>
2	ADMINISTRATOR ATTN DTIC DDA DEFENSE TECHNICAL INFO CTR CAMERON STATION ALEXANDRIA VA 22304-6145
1	COMMANDER ATTN AMCAM US ARMY MATERIEL COMMAND 5001 EISENHOWER AVE ALEXANDRIA VA 22333-0001
1	DIRECTOR ATTN AMSRL OP SD TA US ARMY RESEARCH LAB 2800 POWDER MILL RD ADELPHI MD 20783-1145
3	DIRECTOR ATTN AMSRL OP SD TL US ARMY RESEARCH LAB 2800 POWDER MILL RD ADELPHI MD 20783-1145
1	DIRECTOR ATTN AMSRL OP SD TP US ARMY RESEARCH LAB 2800 POWDER MILL RD ADELPHI MD 20783-1145
2	COMMANDER ATTN SMCAR TDC US ARMY ARDEC PCTNY ARSNL NJ 07806-5000
1	DIRECTOR ATTN SMCAR CCB TL BENET LABORATORIES ARSENAL STREET WATERVLIET NY 12189-4050
1	DIR USA ADVANCED SYSTEMS ATTN AMSAT R NR MS 219 1 R&A OFC AMES RESEARCH CENTER MOFFETT FLD CA 94035-1000

<u>NO. OF COPIES</u>	<u>ORGANIZATION</u>
1	COMMANDER ATTN AMSMI RD CS R DOC US ARMY MISSILE COMMAND REDSTONE ARSNL AL 35898-5010
1	COMMANDER ATTN AMSTA JSK ARMOR ENG BR US ARMY TANK AUTOMOTIVE CMD WARREN MI 48397-5000
1	DIRECTOR ATTN ATRC WSR USA TRADOC ANALYSIS CMD WSMR NM 88002-5502
1	COMMANDANT ATTN ATSH CD SECURITY MGR US ARMY INFANTRY SCHOOL FT BENNING GA 31905-5660
	<u>ABERDEEN PROVING GROUND</u>
2	DIR USAMSAA ATTN AMXSY D AMXSY MP H COHEN
1	CDR USATECOM ATTN AMSTE TC
1	DIR USAERDEC ATTN SCBRD RT
1	CDR USACBD COM ATTN AMSCB CII
1	DIR USARL ATTN AMSRL SL I
5	DIR USARL ATTN AMSRL OP AP L

NO. OF COPIES	ORGANIZATION
1	HQDA (SARD-TR/MS. K. KOMINOS) WASH DC 20310-0103
1	HQDA (SARD-TR/DR. R. CHAIT) WASH DC 20310-0103
1	SDOP/TNI ATTN: L. H. CAVNEY PENTAGON WASHINGTON DC 20301-7100
6	COMMANDER, U.S. ARMY ARDEC ATTN: SMCAR-AET-A, R. DEKLEINE R. KLINE R. BOTTICELLI H. HUDGINS J. GRAU S. KAHN PICATINNY ARSENAL NJ 07806-5001
1	COMMANDER, U.S. ARMY ARDEC ATTN: SMCAR-CCH-V, PAUL VALENTI PICATINNY ARSENAL NJ 07806-5001
2	COMMANDER U.S. ARMY RESEARCH OFFICE ATTN: TECHNICAL LIBRARY D. MANN P.O. BOX 12211 RESEARCH TRIANGLE PARK NC 27709-2211
1	DIRECTOR U.S. ARMY RESEARCH OFFICE ATTN: AMXRO-MCS, MR. K. CLARK P.O. BOX 12211 RESEARCH TRIANGLE PARK NC 27709-2211
1	DIRECTOR U.S. ARMY RESEARCH OFFICE ATTN: AMXRO-RT-IP, LIBRARY SERVICES P.O. BOX 1211 RESEARCH TRIANGLE PARK NC 27709-2211
4	COMMANDER NAVAL RESEARCH LABORATORY ATTN: TECHNICAL LIBRARY CODE 4410, K. KAILASANATH J. BORIS E. ORAN WASHINGTON DC 20375-5000

NO. OF COPIES	ORGANIZATION
1	COMMANDER NAVAL SURFACE WARFARE CENTER ATTN: DR. F. MOORE DAHLGREN VA 22448
7	COMMANDER NAVAL SURFACE WARFARE CENTER ATTN: T. C. SMITH K. RICE S. MITCHELL S. PETERS J. CONSAGA C. GOTZMER TECHNICAL LIBRARY INDIAN HEAD MD 20640-5000
2	COMMANDER NAVAL SURFACE WARFARE CENTER ATTN: CODE R44, DR. A. WARDLAW K24, B402-12, DR. W. YANTA WHITE OAK LABORATORY SILVER SPRING MD 20903-5000
1	USAF WRIGHT AERONAUTICAL LABORATORIES ATTN: AFWAL/FIMG, DR. J. SHANG WPAFB OH 45433-6553
1	AFOSR/NA ATTN: J. TISHKOFF BOLLING AFB DC 20332-6448
3	AIR FORCE ARMAMENT LABORATORY ATTN: AFATL/FXA, STEPHEN C. KORN BRUCE SIMPSON DAVE BELK EGLIN AFB FL 32542-5434
2	WL/MNSH ATTN: R. DRABCZUK D. LITRELL EGLIN AFB FL 32542-5434
1	LOS ALAMOS NATIONAL LABORATORY ATTN: MR. BILL HOGAN MS G770 LOS ALAMOS NM 87545



NO. OF  
COPIES ORGANIZATION

2 DIRECTOR  
SANDIA NATIONAL LABORATORIES  
ATTN: DIV. 1554, DR. W. OBERKAMPF  
DIV. 1554, DR. F. BLOTTNER  
ALBUQUERQUE NM 87185

4 DIRECTOR  
NASA, LANGLEY RESEARCH CENTER  
ATTN: TECH LIBRARY  
MR. D. M. BUSHNELL  
DR. M. J. HEMSCH  
DR. J. SOUTH  
LANGLEY STATION  
HAMPTON VA 23665

2 DIRECTOR  
NASA, LANGLEY RESEARCH CENTER  
ATTN: MS 408,  
W. SCALLION  
D. WITCOFSKI  
HAMPTON VA 23605

6 DIRECTOR  
NASA, AMES RESEARCH CENTER  
ATTN: MS-227-8, L. SCHIFF  
MS-258-1, T. HOLST  
MS-258-1, D. CHAUSSEE  
MS-258-1, M. RAI  
MS-258-1, P. KUTLER  
MS-258-1, P. BUNING  
MOFFETT FIELD CA 94035

1 UNITED STATES MILITARY ACADEMY  
DEPARTMENT OF MECHANICS  
ATTN: LTC ANDREW L. DULL  
WEST POINT NY 10996

1 UNIVERSITY OF CALIFORNIA, DAVIS  
DEPT OF MECHANICAL ENGINEERING  
ATTN: PROF. H. A. DWYER  
DAVIS CA 95616

3 SCIENCE AND TECHNOLOGY INC.  
ATTN: DR. ALAN GLASSER  
MR. BRUCE LOHMAN  
MR. DAVE MAURIZI  
4001 NORTH FAIRFAX DR., NO. 700  
ARLINGTON VA 22203-1618

NO. OF  
COPIES ORGANIZATION

1 MASSACHUSETTS INSTITUTE OF  
TECHNOLOGY  
ATTN: TECH LIBRARY  
77 MASSACHUSETTS AVE.  
CAMBRIDGE MA 02139

1 GRUMANN AEROSPACE CORPORATION  
AEROPHYSICS RESEARCH DEPARTMENT  
ATTN: DR. R. E. MELNIK  
BETHPAGE NY 11714

1 AEDC  
CALSPAN FIELD SERVICE  
ATTN: MS 600, DR. JOHN BENEK  
TULLAHOMA TN 37389

1 VIRGINIA POLYTECHNIC INSTITUTE  
AND STATE UNIVERSITY  
DEPARTMENT OF AEROSPACE AND OCEAN  
ENGINEERING  
ATTN: DR. CLARK H. LEWIS  
BLACKSBURG VA 24061

1 ADVANCED TECHNOLOGY CENTER  
ARVIN/CALSPAN  
AERODYNAMICS RESEARCH DEPARTMENT  
ATTN: DR. M. S. HOLDEN  
P.O. BOX 400  
BUFFALO NY 14225

1 THE PENNSYLVANIA STATE UNIVERSITY  
DEPT OF AEROSPACE ENGINEERING  
ATTN: DR. G. S. DULIKRAVICH  
UNIVERSITY PARK PA 16802

3 THE PENNSYLVANIA STATE UNIVERSITY  
DEPT OF MECHANICAL ENGINEERING  
ATTN: V. YANG  
K. KUO  
C. MERKLE  
UNIVERSITY PARK PA 16802-7501

1 UNIVERSITY OF ILLINOIS AT URBANA  
CHAMPAIGN  
DEPARTMENT OF MECHANICAL AND  
INDUSTRIAL ENGINEERING  
ATTN: DR. J. C. DUTTON  
URBANA IL 61801

NO. OF  
COPIES ORGANIZATION

1 UNIVERSITY OF MARYLAND  
DEPT OF AEROSPACE ENGINEERING  
ATTN: DR. J. D. ANDERSON, JR.  
COLLEGE PARK MD 20742

1 UNIVERSITY OF NOTRE DAME  
DEPT OF AERONAUTICAL AND  
MECHANICAL ENGINEERING  
ATTN: PROF. T. J. MUELLER  
NOTRE DAME IN 46556

1 UNIVERSITY OF TEXAS  
DEPT OF AEROSPACE ENGINEERING  
MECHANICS  
ATTN: DR. D. S. DOLLING  
AUSTIN TX 78712-1055

1 UNIVERSITY OF DELAWARE  
DEPT OF MECHANICAL ENGINEERING  
ATTN: DR. JOHN MEAKIN, CHAIRMAN  
NEWARK DE 19716

1 ARROW TECHNOLOGY ASSOCIATES, INC.  
ATTN: W. HATHAWAY  
P.O. BOX 4218  
SOUTH BURLINGTON VT 05401-0042

1 PAUL GOUGH ASSOCIATES, INC.  
ATTN: P. S. GOUGH  
1048 SOUTH ST.  
PORTSMOUTH NH 03801-5423

2 PRINCETON COMBUSTION RESEARCH  
LABORATORIES, INC.  
ATTN: N. MER  
N. A. MESSINA  
PRINCETON CORPORATE PLAZA  
11 DEERPARK DR., BLDG. IV, SUITE 119  
MONMOUTH JUNCTION NJ 08852

1 ROCKWELL INTERNATIONAL  
ROCKETDYNE DIVISION  
ATTN: BA08, R. B. EDELMAN  
6633 CANOGA AVE.  
CANOGA PARK CA 91303-2703

2 ROCKWELL INTERNATIONAL SCIENCE  
CENTER  
ATTN: DR. S. CHAKRAVARTHY  
DR. S. PALANISWAMY  
1049 CAMINO DOS RIOS  
THOUSAND OAKS CA 91360

NO. OF  
COPIES ORGANIZATION

1 VERITAY TECHNOLOGY, INC.  
ATTN: E. FISHER  
4845 MILLERSPORT HIGHWAY  
EAST AMHEREST NY 14501-0305

ABERDEEN PROVING GROUND

31 DIR, USARL  
ATTN: AMSRL-WT-P, MR. ALBERT HORST  
AMSRL-WT-PB,  
DR. E. SCHMIDT  
MR. B. GUIDOS  
DR. P. PLOSTINS  
DR. J. SAHU  
MR. P. WEINACHT  
DR. G. COOPER  
AMSRL-WT, DR. A. BARROWS  
AMSRL-WT-PD, DR. B. BURNS  
AMSRL-WT-PA,  
DR. T. MINOR  
MR. M. NUSCA (7 CP)  
MS. G. WREN  
DR. T. COFFEE  
MR. J. DESPIRITO  
DR. D. KOOKER  
MR. D. KRUCZYNSKI  
DR. G. KELLER  
DR. F. LIBERATORE  
AMSRL-WT-W, DR. C. MURPHY  
AMSRL-WT-WB, DR. W. D'AMICO  
AMSRL-WT-NC,  
MS. D. HISLEY  
MR. R. LOTTERO  
DR. K. OPALKA  
AMSRL-CI-C,  
DR. W. STUREK  
DR. N. PATEL

3 DIR USAERDEC  
ATTN SCBRD-RTB,  
MR. D. PALUGHI  
MR. L. BICKFORD  
DR. S. THOMPSON

## USER EVALUATION SHEET/CHANGE OF ADDRESS

This Laboratory undertakes a continuing effort to improve the quality of the reports it publishes. Your comments/answers to the items/questions below will aid us in our efforts.

1. ARL Report Number ARL-TR-663 Date of Report January 1995

2. Date Report Received \_\_\_\_\_

3. Does this report satisfy a need? (Comment on purpose, related project, or other area of interest for which the report will be used.) \_\_\_\_\_  
\_\_\_\_\_  
\_\_\_\_\_

4. Specifically, how is the report being used? (Information source, design data, procedure, source of ideas, etc.) \_\_\_\_\_  
\_\_\_\_\_  
\_\_\_\_\_

5. Has the information in this report led to any quantitative savings as far as man-hours or dollars saved, operating costs avoided, or efficiencies achieved, etc? If so, please elaborate. \_\_\_\_\_  
\_\_\_\_\_  
\_\_\_\_\_

6. General Comments. What do you think should be changed to improve future reports? (Indicate changes to organization, technical content, format, etc.) \_\_\_\_\_  
\_\_\_\_\_  
\_\_\_\_\_  
\_\_\_\_\_

### CURRENT ADDRESS

\_\_\_\_\_  
Organization

\_\_\_\_\_  
Name

\_\_\_\_\_  
Street or P.O. Box No.

\_\_\_\_\_  
City, State, Zip Code

7. If indicating a Change of Address or Address Correction, please provide the Current or Correct address above and the Old or Incorrect address below.

### OLD ADDRESS

\_\_\_\_\_  
Organization

\_\_\_\_\_  
Name

\_\_\_\_\_  
Street or P.O. Box No.

\_\_\_\_\_  
City, State, Zip Code

(Remove this sheet, fold as indicated, tape closed, and mail.)  
(DO NOT STAPLE)

---

DEPARTMENT OF THE ARMY

OFFICIAL BUSINESS



NO POSTAGE  
NECESSARY  
IF MAILED  
IN THE  
UNITED STATES

**BUSINESS REPLY MAIL**  
FIRST CLASS PERMIT NO 0001, APG, MD

Postage will be paid by addressee

**Director**  
**U.S. Army Research Laboratory**  
**ATTN: AMSRL-OP-AP-L**  
**Aberdeen Proving Ground, MD 21005-5066**

